MLN4924, a NEDD8-activating enzyme inhibitor, is active in diffuse large B-cell lymphoma models: rationale for treatment of NF-κB–dependent lymphoma

*Michael A. Milhollen,[1] *Tary Traore,[1] Jennifer Adams-Duffy,[1] Michael P. Thomas,[1] Allison J. Berger,[1] Lenny Dang,[1] Lawrence R. Dick,[1] James J. Garnsey,[1] Erik Koenig,[1] Steven P. Langston,[1] Mark Manfredi,[1] Usha Narayanan,[1] Mark Rolfe,[1] Louis M. Staudt,[2] Teresa A. Soucy,[1] Jie Yu,[1] Julie Zhang,[1] Joseph B. Bolen,[1] and Peter G. Smith[1]

[1]Discovery, Millennium Pharmaceuticals, Inc, Cambridge, MA; and [2]Metabolism Branch, Center for Cancer Research, National Cancer Institute, National Institutes of Health, Bethesda, MD

MLN4924 is a potent and selective small molecule NEDD8-activating enzyme (NAE) inhibitor. In most cancer cells tested, inhibition of NAE leads to induction of DNA rereplication, resulting in DNA damage and cell death. However, in preclinical models of activated B cell–like (ABC) diffuse large B-cell lymphoma (DLBCL), we show that MLN4924 induces an alternative mechanism of action. Treatment of ABC DLBCL cells with MLN4924 resulted in rapid accumulation of pIκBα, decrease in nuclear p65 content, reduc- tion of nuclear factor-κB (NF-κB) tran- scriptional activity, and G$_1$ arrest, ulti- mately resulting in apoptosis induction, events consistent with potent NF-κB path- way inhibition. Treatment of germinal- center B cell–like (GCB) DLBCL cells re- sulted in an increase in cellular Cdt-1 and accumulation of cells in S-phase, consis- tent with cells undergoing DNA rerepli- cation. In vivo administration of MLN4924 to mice bearing human xenograft tumors of ABC- and GCB-DLBCL blocked NAE pathway biomarkers and resulted in com- plete tumor growth inhibition. In primary human tumor models of ABC-DLBCL, MLN4924 treatment resulted in NF-κB pathway inhibition accompanied by tu- mor regressions. This work describes a novel mechanism of targeted NF-κB pathway modulation in DLBCL and pro- vides strong rationale for clinical devel- opment of MLN4924 against NF-κB– dependent lymphomas. (*Blood*. 2010; 116(9):1515-1523)

Introduction

MLN4924 is a potent and selective small-molecule inhibitor of NEDD8-activating enzyme (NAE) that is currently in phase 1 clinical trials.[1-3] NAE plays an essential role in regulating the activity of a subset of ubiquitin E3 ligases, the cullin-RING ligases (CRLs), which are responsible for regulating destruction of many intracellular proteins.[4] NAE activates the small ubiquitin-like molecule NEDD8 as the first step in the neddylation cascade.[5] NAE hydrolyzes adenosine triphosphate (ATP) to adenylate NEDD8 at its C-terminus and transfers NEDD8 from the adenyl group to a specific cysteine within NAE. The activated NEDD8 is then transferred to the active-site cysteine of Ubc12 or UBE2F the E2s specific for the NEDD8 pathway. Finally, NEDD8 is conjugated on a conserved lysine near the C-terminal end of a cullin protein; this covalent modification is required for the cullin complex to recruit a ubiquitin-charged E2 protein facilitating polyubiquitination of proteins, targeting them for proteasomal degradation. Thus, NAE plays a key role in regulating the levels (and therefore the function) of a subset of proteins.

Many of the proteins that are substrates for CRL-mediated polyubiquitination have key roles in cell-cycle progression and signal transduction, making NAE inhibition an attractive target for anticancer therapy. MLN4924 potently inhibits NAE in vitro, resulting in inhibition of CRL neddylation and an increase in levels of CRL substrate proteins (eg, Cdt-1, Nrf-2).[3] The primary mechanism of action of NAE inhibition in many cell types is induction of DNA rereplication because of blocking degradation of Cdt-1, a critical factor required for licensing origins of DNA replication.[3] Dysregulation of Cdt-1 activity leads to DNA rerepli- cation.[6,7] For example, overexpression of Cdt-1 and Cdc6 induces DNA rereplication, activates DNA damage repair pathways, and induces cell death.[7] Induction of DNA rereplication by MLN4924 results in S-phase accumulation, DNA-damage responses, and cell death[3] (M.A.M., U.N., T.A.S., P. Veiby, P.G.S., B. Amidon, manuscript in preparation). Similar effects were observed in human tumor xenografts where MLN4924 inhibited NAE in vivo leading to tumor growth inhibition.[3]

The nuclear factor-κB (NF-κB) signaling pathway plays a key role in many aspects of cancer initiation and progression through transcriptional control of genes involved in growth, angiogenesis, antiapoptosis, invasiveness, and metastasis.[8] Regulation of NF-κB signaling occurs at many levels, one of which is through the regulation of protein turnover by the action of CRLs. Under normal conditions, NF-κB transcription factors are maintained in an inactive state by binding to IκB proteins. In canonical NF-κB signaling, IκBα binds to p50-p65, sequesters the transcription factors in the cytoplasm rendering them inactive. On stimulation of the IKK complex, IκBα is phosphorylated at Ser32 and Ser36, resulting in its polyubiquitination and degradation,[9-11] thus result- ing in nuclear accumulation of the complex and transcription of NF-κB target genes. Polyubiquitination of IκBα is regulated by CRL1$^{\beta TRCP}$, which in turn is tightly regulated by NAE.[12] In noncanonical NF-κB signaling, processing of p105 to p50 and

---

p100 to p52 is also controlled by CRL1$^{\beta TRCP}$.[13,14] Therefore, both canonical and noncanonical NF-κB signaling requires NAE activity. Thus, NAE inhibition by MLN4924 represents a novel approach to inhibit NF-κB and may provide a targeted therapeutic strategy for the treatment of cancers in which NF-κB signaling is important.

One such cancer is diffuse large B-cell lymphoma (DLBCL), a non-Hodgkin lymphoma that has been classified into several distinct genetic subgroups based on cDNA microarray analysis.[15] Activated B cell–like (ABC)–DLBCL has the poorest prognosis and remains an indication with unmet medical needs where patients have elevated NF-κB gene expression signature.[16] Inhibition of NF-κB using shRNA, expression of an IκB-super repressor, or treatment with small-molecule IKK inhibitors has been shown to be selectively toxic to ABC-DLBCL but not germinal center B-cell-like (GCB)–DLBCL cells.[16-18] Inhibition of IKK in these cells leads to G_1-arrest and induction of apoptosis. These studies demonstrate the dependence of ABC-DLBCL on NF-κB signaling for survival and offer a compelling clinical rationale for the use of NF-κB inhibitors in this disease.

In this report, we investigate the effect of MLN4924 as a novel NF-κB targeted therapy in DLBCL cells and mouse xenograft models. We show that MLN4924 is a potent inhibitor of NF-κB pathway in vitro and in vivo in NF-κB–dependent DLBCLs, resulting in induction of apoptosis and tumor regressions. In addition, we show that MLN4924 also has potent antitumor activity in non–NF-κB–dependent DLBCLs through induction of DNA rereplication, independent of NF-κB status. These studies support the potential for broad activity of MLN4924 in hematologic malignancies, with a rationale for targeted therapy in NF-κB–dependent lymphomas, and serve as the basis for the ongoing phase 1 evaluation of MLN4924 in hematologic malignancies.

Methods

Cell viability assay

OCI-Ly3, OCI-Ly7, OCI-Ly10, OCI-Ly19, HBL1, L1236, and U2932 cells were a kind gift from Lou Staudt (National Cancer Institute, Bethesda, MD). All other cell viability assays were performed by Southern Research. Cell suspensions were seeded at 3000 to 8000 cells per well in 96-well culture plates and incubated overnight at 37°C. Compounds were added to the cells in complete growth media and incubated for 72 hours at 37°C. Cell number was quantified using the ATPlite assay (PerkinElmer Life and Analytical Sciences).

Western blot analysis of cultured cells

DLBCL cells grown in 6-well cell culture dishes were treated with 0.1% dimethyl sulfoxide (DMSO; control) or MLN4924 for the times indicated. Whole-cell extracts were prepared and analyzed by immunoblotting. For analysis of E2-UBL thioester levels, lysates were fractionated by nonreducing sodium dodecyl sulfate–polyacrylamide gel electrophoresis and immunoblotted with polyclonal antibodies to Ubc12 (generated by Millennium). For analysis of other proteins, lysates were fractionated by reducing sodium dodecyl sulfate–polyacrylamide gel electrophoresis and probed with primary antibodies as follows: Cdt-1, NEDD8, and Chk1 (Ser 317, Millennium), pIκBα (Ser 32), pp105 (Ser 933), p105/50, pH3 (Ser 10), pH2AX (Ser 139), cleaved PARP and cleaved caspase-3 (Cell Signaling), and Nrf-2 (Epitomics). Secondary horseradish peroxidase–labeled antibodies to rabbit immunoglobulin G (IgG) or mouse IgG (Santa Cruz Biotechnology) were used as appropriate. Blots were developed with enhanced chemiluminescence reagent (GE Healthcare).

Cell-cycle analysis

Logarithmically growing DLBCL cells were incubated with either MLN4924 or DMSO for the times indicated. Analysis was performed as described previously.[3]

Nuclear p65 quantitation

Logarithmically growing DLBCL cells were incubated with increasing concentrations of MLN4924 or DMSO as indicated for 4 hours. The nuclear extract was prepared (Nuclear Extract Kit, Active Motif) and protein concentration determined by the Bradford method. After incubating nuclear extract or p65 standard in oligonucleotide-coated assay plate (TransAM kit, Active Motif) for 1 hour at room temperature, the plate was washed 3 times with wash buffer, and anti-p65 antibody (Santa Cruz Biotechnology) was added to each well. The plate was incubated for 1 hour at room temperature, washed 3 times with wash buffer and once with Delfia Wash Buffer (PerkinElmer Life and Analytical Sciences). Delfia Eu-N1–labeled secondary antibody (PerkinElmer Life and Analytical Sciences) was then added to each well with Delfia Assay Buffer (PerkinElmer Life and Analytical Sciences). The plate was incubated for 1 hour; and after repeated washes, Delfia Enhancement Solution (PerkinElmer Life and Analytical Sciences) was added. The plate was measured using a time-resolved fluorometer, and relative fluorescent units were converted to picograms of p65 using the standard curve and then normalized by total amount of protein loaded per well.

BrdU incorporation assay

Logarithmically growing DLBCL cells were incubated with increasing concentrations of MLN4924 or DMSO as indicated for 3.5 hours and were pulsed with 10μM bromodeoxyuridine (BrdU; BD Biosciences) for 30 minutes (total MLN4924 incubation time of 4 hours). Cells were then collected and fixed at 4°C in 70% ethanol. Cells were washed in cold phosphate-buffered saline (PBS), pelleted, and resuspended in 1 mL of 2N HCl for 20 minutes and with PBS. Cell pellets were then resuspended in 0.5 mL 0.1M sodium borate ($Na_2B_4O_7$), pH 8.5, for 2 minutes, washed in PBS, and the resultant cell pellet was resuspended in 20 μL of anti-BrdU monoclonal antibody (BD Biosciences) and incubated in the dark for 20 minutes at room temperature. After incubation, cells were washed with PBS and resuspended in 0.5 mL PBS containing 10 μg/mL propidium iodide for 1 hour protected from light. Labeled cells were analyzed for propidium iodide and BrdU staining on a BD Biosciences FACSCalibur flow cytometer using Winlist software v5.0 (Verity).

Quantitative RT-PCR (in vitro/in vivo)

DLBCL cells grown in 6-well cell culture dishes were treated with 0.1% DMSO (control) or MLN4924 for the times indicated. Cells were pelleted and snap-frozen on dry ice before extraction of DNAase-treated RNA using QIAGEN reagents. cDNA synthesis and quantitative reverse-transcribed polymerase chain reaction (RT-PCR) were performed using ABI Gene Expression Assays (supplemental Table 1, available on the *Blood* Web site; see the Supplemental Materials link at the top of the online article), reagents, and ABI PRISM 7900HT Sequence Detection Systems (Applied Biosystems) using the following cycle conditions: hold at 50°C for 2 minutes for AmpErase UNG activation, then 95.0°C for 10 minutes to activate DNA polymerase, and then run 40 two-part cycles of 95.0°C for 15 seconds and 60.0°C for 1 minute. Relative mRNA expression quantitation was derived using the comparative Ct method (Applied Biosystems). The ΔCt (dCt) was calculated using the average Ct of control genes B2M (Hs99999907_m1) and 18S (Hs99999901_s1). The ΔΔCt (ddCt) was calculated by subtracting the dCt value for the treated sample from the dCt value of the experimental control sample following equation: ddCt = dCt(control) − dCt(treated). For analysis of mRNA levels in xenograft samples, tumor fragments were harvested, snap-frozen on dry ice, and subjected to RT-PCR analysis as described in this section.

Tumor xenograft efficacy experiments

Female CB.17 SCID mice (Taconic Farms) were used for in vivo studies with OCI-Ly10, OCI-Ly19, and OCI-LY19-luc cells. Female SCID NOD mice (Taconic Farms) were used for in vivo studies with PHTX22L model. All animals were housed and handled in accordance with the Guide for the Care and Use of

Laboratory Animals. For subcutaneous xenograft studies, mice were inoculated with 4×10^6 OCI-Ly10 or OCI-Ly19 cells with Matrigel (BD Biosciences) in the right flank, and tumor growth was monitored with caliper measurements. When the mean tumor volume reached approximately 200 mm³, animals were dosed subcutaneously with vehicle (10% cyclodextrin) or MLN4924. Inhibition of tumor growth (T/C, average treated tumor volume/average control tumor volume) was calculated on the last day of treatment. For disseminated xenograft studies, mice were inoculated with 1×10^6 OCI-Ly19-luc cells (OCI-Ly19-luc cells are a stable cell line generated after retroviral infection of OCI-Ly19 cells with the luciferase transgene under the control of the cytomegalovirus promoter) intravenously, and tumor burden was monitored with xenogen imaging (Taconic Farms).

Pharmacodynamic marker analysis

Mice bearing DLBCL tumors of 300 to 500 mm³ were administered a single MLN4924 dose; and at the indicated times, tumors were excised and extracts prepared. The relative levels of NEDD8-cullin, pIκBα, and Nrf-2 were estimated by quantitative immunoblot analysis (Li-Cor Odyssey system) using Alexa 680–labeled anti-IgG (Invitrogen) as the secondary antibody. Cleaved caspase 3 was detected using enhanced chemiluminescence immunoblotting.

Results

MLN4924 inhibits NAE, prevents cell growth, and generates distinct cell-cycle profiles in DLBCL cells

Two cell lines representative of ABC-DLBCL (OCI-Ly10, OCI-Ly3) and 2 representative of GCB-DLBCL (OCI-Ly19, OCI-Ly7) were used.[15,16]

Potent inhibition of cell viability was observed across 17 lymphoma cell lines tested in an ATPlite viability assay, with EC_{50} values of 10 to 244nM (supplemental Table 2). Interestingly, MLN4924 inhibited viability in GCB-DLBCL cell lines (OCI-Ly19, OCI-Ly7), which have been previously shown to be insensitive to small-molecule IKK inhibitors.[17] Because there was no discrimination in sensitivity of ABC- and GCB-DLBCL cells, we hypothesized that in ABC-DLBCL NAE inhibition may primarily result in NF-κB pathway inhibition, whereas in GCB-DLBCL the mechanism of action may be the result of DNA rereplication.[3] To confirm NAE inhibition in both types of DLBCL cells, an anti-NEDD8 antibody was used to detect NEDD8 conjugation to Ubc12 (an E2 for NEDD8) and the cullin proteins. Cells were exposed to increasing concentrations of MLN4924 for 24 hours; a dose-dependent decrease of Ubc12-NEDD8 thioester and NEDD8-cullin conjugate levels was observed in all cells (Figure 1A). These data show that the neddylation pathway was inhibited to similar levels in ABC- and GCB-DLBCL cells.

IκBα superrepressor transfection and small-molecule IKK inhibition induce G_1-phase cell-cycle arrest in OCI-Ly10 and OCI-Ly3 cells.[16,17] We recently reported that NAE inhibition results in an accumulation of cells in S-phase.[3] To determine whether similar effects were seen with NAE inhibition in DLBCL, cells were exposed to increasing concentrations of MLN4924 for 24 hours and cell-cycle profiles analyzed by flow cytometry. In OCI-Ly10 and OCI-Ly3 cells, a prominent G_1 phenotype was observed with a proportion of cells sub-G_1 indicative of apoptosis (Figure 1B). In contrast, OCI-Ly19 and OCI-Ly7 cells demonstrated an accumulation in S-phase and some cells containing more than 4N DNA content. Quantitation of cell-cycle distributions of DLBCL cells in response to MLN4924 confirmed marked differences between OCI-Ly10 and OCI-Ly3 cells compared with OCI-Ly19 and OCI-Ly7 cells (supplemental Figure 1). These data

suggested that ABC-DLBCL cells are affected differently by NAE inhibition, with the predominant phenotype being consistent with NF-κB signaling inhibition, whereas GCB-DLBCL cells were undergoing DNA rereplication.

MLN4924 induces apoptosis through inhibition of NF-κB signaling in ABC-DLBCL and induction of DNA rereplication in GCB-DLBCL

OCI-Ly10 and OCI-Ly19 cells were exposed to MLN4924 concentrations that elicit 50% and 90% inhibition of viability in a 72-hour ATPlite assay, as well as a higher concentration of 1μM (Figure 2A-B). Cells were isolated at indicated time points after addition of MLN4924, and NAE inhibition was evaluated. A dose-response was observed in OCI-Ly10 cells as demonstrated by inhibition of NEDD8-cullin levels (Figure 2A). Rapid inhibition of pathway activity was observed as early as 1 hour after addition of MLN4924, in agreement with effects observed in HCT-116 cells.[3] Consistent with the constitutively active NF-κB signaling pathway in OCI-Ly10 cells, accumulation of pIκBα (Ser32) was also observed as early as 1 hour after treatment and before (and at lower MLN4924 concentrations) elevation of Cdt-1. Elevation of pIκBα and Cdt-1 was sustained for 8 hours after treatment, whereupon evidence of DNA damage was detected as shown by phosphorylation of the ATM substrate pChk-1 (Ser317) and p-H2AX (Ser 139). In addition, cleavage of caspase-3 was observed as early as 4 hours after treatment at 1μM and more robustly at 8 hours, showing that apoptosis induction is rapid in OCI-Ly10 cells. Dose- and time-dependent NAE inhibition was also observed in OCI-Ly19 cells, with inhibition of NEDD8-cullin conjugation occurring as early as 1 hour after incubation with MLN4924 (Figure 2B). In OCI-Ly19 cells, Cdt-1 elevation occurred earlier and at lower MLN4924 concentrations than pIκBα elevation, supporting the hypothesis that the primary mechanism of action of MLN4924 in this setting is DNA rereplication. In contrast to OCI-Ly10 cells, Cdt-1 elevation was sustained for at least 24 hours and pChk-1 and pH2AX activation occurred later, at 16 and 24 hours. Interestingly, no activation of caspase-3 cleavage was detected at 24 hours; however, at 48 hours, robust cleavage of caspase-3 was evident, indicating that OCI-Ly19 cells also undergo apoptosis in response to NAE inhibition (Figure 2B; supplemental Figure 2). Supportive evidence from studies using OCI-Ly3 (ABC-DLBCL) and OCI-Ly7 (GCB-DLBCL) cells is provided in supplemental Figure 3; pIκBα accumulation occurred more robustly in OCI-Ly3 than OCI-Ly7 cells at 4 hours and activation of apoptosis was seen in OCI-Ly3 but not OCI-Ly7 cells at 24 hours, whereas robust accumulation of Cdt-1 was observed in OCI-Ly7 cells but not in OCI-Ly3 cells. To confirm OCI-Ly10 cells were not rereplicating, BrdU incorporation assays were performed at the 4-hour time point, when Cdt-1 levels were highest after MLN4924 treatment (Figure 2A). Increased BrdU incorporation occurs in cells actively undergoing DNA rereplication.[7,19] BrdU incorporation was unchanged in MLN4924-treated OCI-Ly10 cells (supplemental Figure 4).

Accumulation of cytoplasmic pIκBα should retain NF-κB subunits in the cytoplasm, resulting in decreased nuclear localization of p50-p65. We used an enzyme-linked immunosorbent assay to measure nuclear p65 levels in OCI-Ly10 and OCI-Ly19 cells after 4-hour incubation with increasing MLN4924 concentrations. A dose-dependent decrease in nuclear p65 levels was observed in OCI-Ly10 cells, whereas no change was observed in OCI-Ly19 cells (Figure 2C). Similar data were observed in OCI-Ly3 (ABC-DLBCL) and OCI-Ly7 (GCB-DLBCL) cells (supplemental Figure 5). Notably, the EC_{50} (~ 25nM) for inhibition of nuclear p65 levels
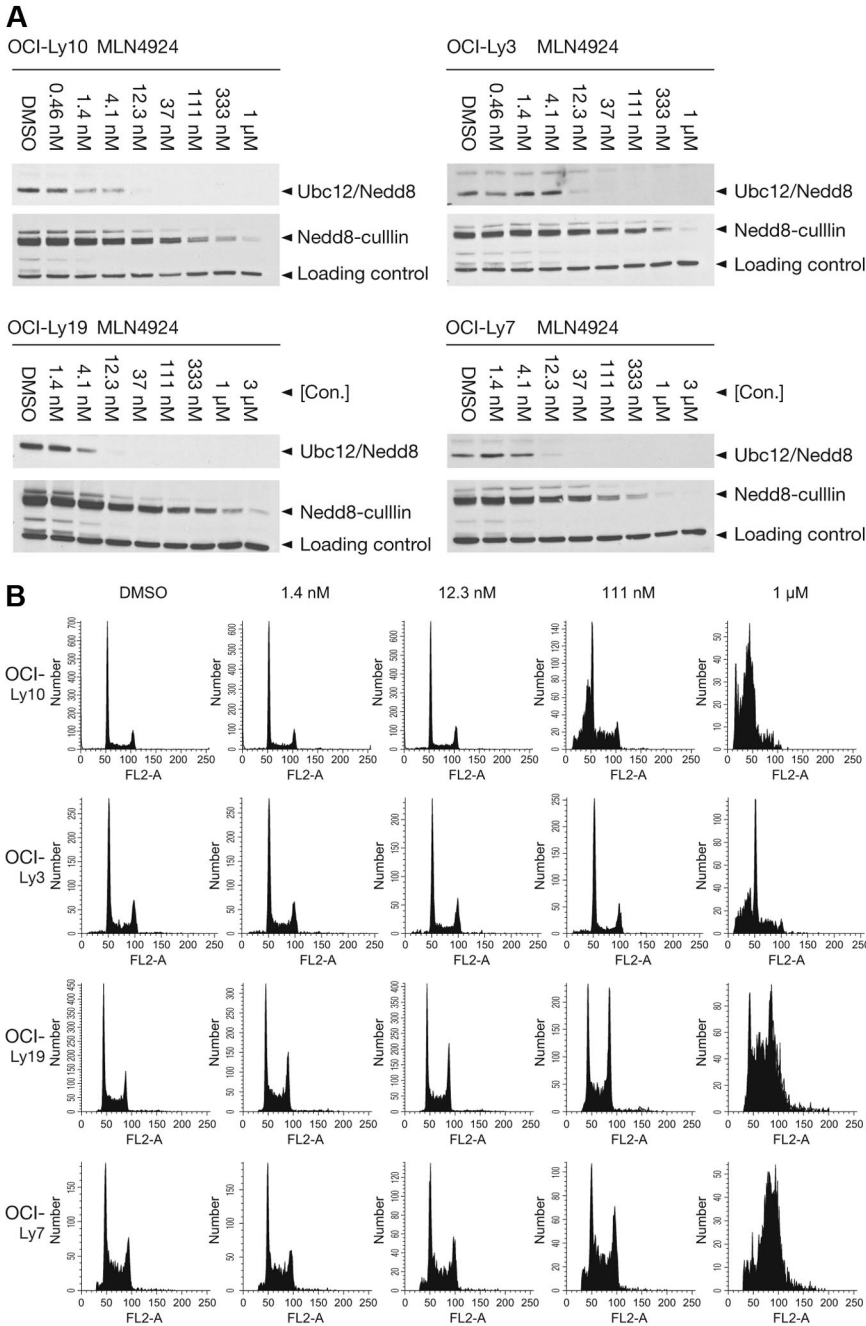
A

B

Figure 1. MLN4924 is a potent inhibitor of NAE and induces distinct cell-cycle profiles analyzed by flow cytometry in ABC- and GCB-DLBCL cell lines. OCI-Ly10, OCI-Ly3, OCI-Ly19, and OCI-Ly7 cells were treated with MLN4924 for 24 hours. (A) Inhibition of NAE was assessed by immunoblot analysis of Ubc12-NEDD8 thioester and cullin-NEDD8 levels, respectively. The nonspecific band serves as the loading control. (B) DNA profiles were analyzed by propidium iodide staining and flow cytometry.

in OCI-Ly10 cells was similar to the EC_{50} (11nM) for inhibition of viability (supplemental Table 2), suggesting an association between NF-κB pathway effects and cell viability for MLN4924.

TaqMan low-density arrays were used to measure the levels of NF-κB target genes. We found that MLN4924 down-regulated NF-κB target genes (eg, *TNFα*, *IRF4*, *PIM1*, *IκBα*, and *CXCL10*) in OCI-Ly10 cells in a dose- and time-dependent manner (Figure 2D). At EC_{90} concentrations of MLN4924 that inhibit OCI-Ly10 viability, a significant decrease in transcript levels of NF-κB target genes was noted as early as 3 to 6 hours after treatment. In contrast, minimal changes in NF-κB target gene expression were detected in OCI-Ly19 cells, consistent with the low level of NF-κB activity and lack of p65 redistribution.

These data demonstrate that MLN4924 inhibits NAE and leads to cell death in both OCI-Ly10 and OCI-Ly19 cells. In OCI-Ly10 cells, the primary mechanism of action is probably the result of NF-κB signaling

inhibition, as evidenced by increased pIκBα levels, decreased nuclear p65, and inhibition of NF-κB target gene transcription. In OCI-Ly19 cells, the primary mechanism of action is probably induction of DNA rereplication, as evidenced by elevated Cdt-1 levels, accumulation of cells in S-phase (with evidence of > 4N DNA content), and no effect on NF-κB target gene transcription.

MLN4924 inhibits NAE in ABC- and GCB-DLBCL human xenografts grown in mice

To determine the effects of NAE inhibition by MLN4924 in vivo, OCI-Ly10 and OCI-Ly19-luc cells were grown as subcutaneous xenografts in CB.17 SCID mice. OCI-Ly19-luc cells are a stable cell line generated after infection with a retrovirus expressing the luciferase transgene under the control of the cytomegalovirus promoter. Mice received a single subcutaneous dose of 10, 30, or

Figure 2. MLN4924 induces apoptosis through inhibition of NF-κB signaling in ABC-DLBCL and induction of DNA rereplication in GCB-DLBCL. OCI-Ly10 (A) and OCI-Ly19 (B) cells were treated with EC_{50}, EC_{90}, and 1μM concentrations of MLN4924 for 1, 2, 4, 8, 16, and 24 hours. Cell lysates were immunoblotted for NEDD8-cullin, phosphorylated IκBα (Ser32), Cdt-1, phosphorylated Chk1 (Ser317), phosphorylated H2AX (SER139, cleaved (Clvd) caspase 3, and tubulin. (C) OCI-Ly10 and OCI-Ly19 cells were treated with increasing concentrations of MLN4924 for 4 hours. The nuclear fraction was prepared and subjected to enzyme-linked immunosorbent assay–based quantitation of p65 levels. (D) OCI-Ly10 and OCI-Ly19 cells were treated with EC_{90} concentrations of MLN4924 for 1, 3, 6, 12, and 24 hours, and quantitative RT-PCR was performed to measure levels of NF-κB target gene transcripts.
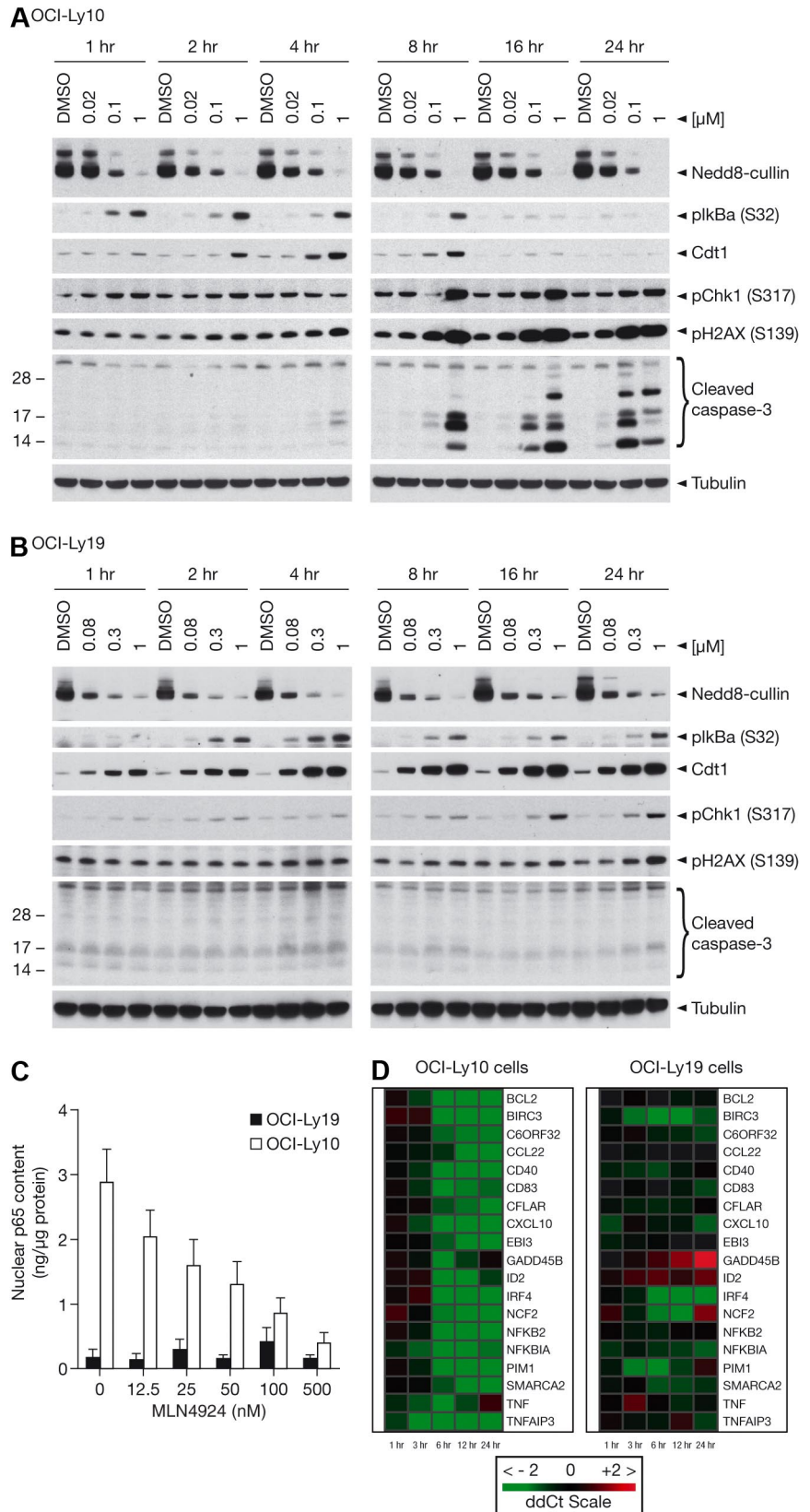
60 mg/kg MLN4924; tumor samples were harvested over 24 hours to assess pharmacodynamic response to MLN4924. Tumor lysates were assessed for modulation of NEDD8-cullin levels, the CRL substrates pIκBα, Nrf-2, and cleaved caspase-3 protein levels (Figure 3). Similar dose- and time-dependent inhibition of NEDD8-

cullin levels was observed in OCI-Ly10 and OCI-Ly19-luc xenografts, with the maximal effect occurring 1 to 2 hours after dose (Figure 3A,E). Dose- and time-dependent increases in Nrf-2 levels were observed in both xenografts, with peak elevation occurring 2 to 4 hours after dose (Figure 3B,F). These data suggest that NAE
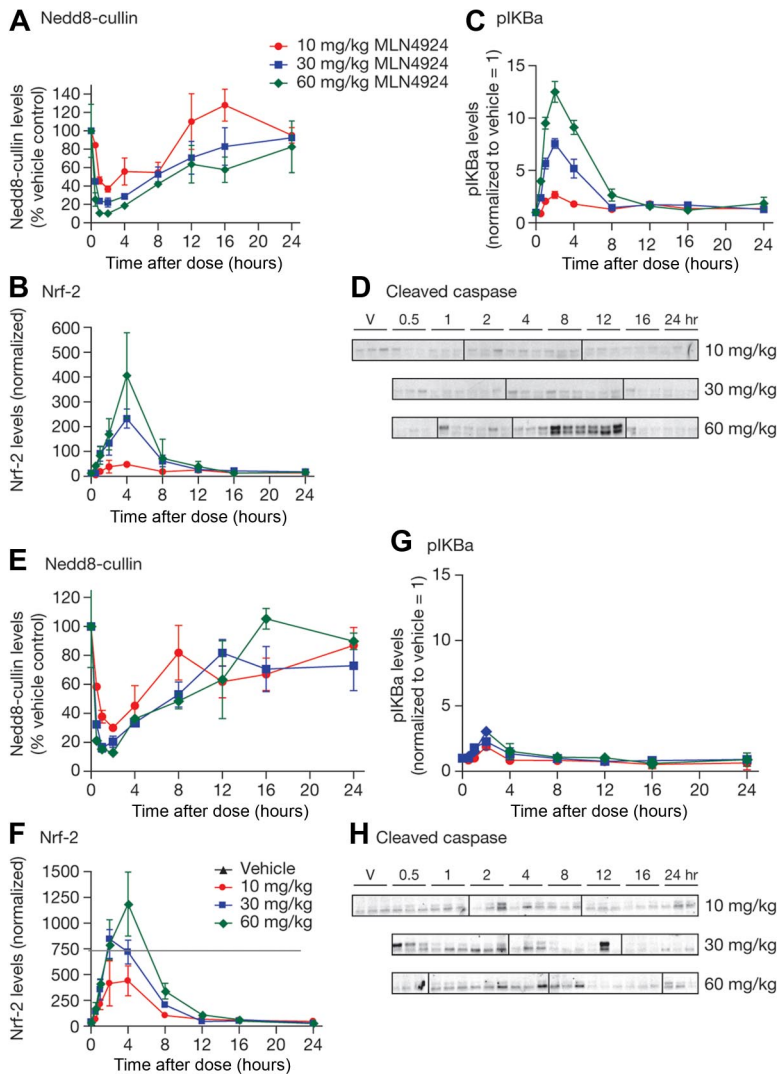
Figure 3. MLN4924 inhibits NAE in human xenograft models of DLBCL. CB.17 SCID mice bearing OCI-Ly10 (A-D) and OCI-Ly19-luc (E-H) xenografts were administered a single subcutaneous dose of vehicle or MLN4924 at 10, 30, or 60 mg/kg. Tumors were excised at the indicated times and NEDD8-cullin conjugate levels (A,E), relative Nrf-2 protein levels (B,F), and relative pIκBα levels (C,G) were measured in the tumor lysates (20 μg protein per lane) by quantitative immunoblot analysis. Units are arbitrary. In panel F, the assay has a linear standard curve up to 750 units. Western blotting was also performed to analyze levels of cleaved caspase 3 after a single subcutaneous dose of 60 mg/kg (D,H). Vertical lines have been inserted to indicate repositioned gel lanes.

was inhibited to equivalent levels and for a similar length of time in OCI-Ly10 and OCI-Ly19-luc xenografts. A difference was noted in the pharmacodynamic response of pIκBα; in OCI-Ly10 xenografts, a dose- and time-dependent increase in pIκBα levels was observed after MLN4924 treatment, with peak elevation occurring 2 hours after dose and levels returning to baseline at 8 hours after dose (Figure 3C). In contrast, in OCI-Ly19-luc xenografts, there was only a modest elevation compared with OCI-Ly10 xenografts (Figure 3G). A consequence of inhibiting NAE and NF-κB signaling in OCI-Ly10 xenografts was the induction of apoptosis 8 to 12 hours after a single dose of 60 mg/kg MLN4924, as evidenced by detection of cleaved caspase-3 (Figure 3D). No increase in cleaved caspase-3 levels was observed in OCI-Ly19-luc xenografts up to 24 hours after dosing (Figure 3H). NF-κB signaling inhibition was confirmed in OCI-Ly10 xenografts by decreases in mRNA levels of NF-κB target genes after a single dose of MLN4924 (supplemental Figure 6).

These results demonstrate that MLN4924 inhibits NAE in both ABC- and GCB-DLBCL xenografts. In ABC-DLBCL xenografts, NAE inhibition was accompanied by elevation of pIκBα levels, inhibition of NF-κB target gene transcription, and a subsequent induction of apoptosis. Apoptosis induction was not observed after a single dose in GCB-DLBCL, suggesting an acute sensitivity of ABC-DLBCL xenografts because of perturbation of the NAE pathway in vivo.

MLN4924 inhibits DLBCL xenograft growth resulting in tumor regressions in ABC-DLBCL

To examine the antitumor activity of MLN4924 in vivo, OCI-Ly10 and OCI-Ly19 cells were grown as subcutaneous xenografts in CB.17 SCID mice. Once tumors were established (~ 200 mm³), subcutaneous administration of MLN4924 occurred twice daily at doses of 10, 30, or 60 mg/kg using various schedules (Figure 4). Tumor growth inhibition was assessed on the last day of study. In OCI-Ly10 xenografts a dose-dependent inhibition of tumor growth was observed, with complete inhibition occurring at 30 mg/kg twice daily (T/C = 0.27) and tumor regressions observed at 60 mg/kg twice daily (T/C = 0.08, Figure 4A). Less frequent administration of MLN4924 60 mg/kg twice daily also resulted in tumor regressions; 2 cycles of 5 days of treatment followed by 5 days free of treatment resulted in 10 of 10 tumor regressions. Thus, tumor regressions are observed at the maximum tolerated dose (MTD, 60 mg/kg twice daily for 21 days), but also on schedules less than the MTD. These data show that MLN4924 does not require daily administration to exert potent antitumor activity in OCI-Ly10 xenografts.

Dose-dependent tumor growth inhibition was also observed in OCI-Ly19 xenografts, with complete tumor growth inhibition (T/C = 0.10) occurring at 60 mg/kg twice daily (Figure 4B). Similar to the OCI-Ly10 model, continuous daily dosing was not

Figure 4. MLN4924 inhibits the growth of human xeno-graft models of DLBCL. CB.17 SCID mice bearing OCI-Ly10 (A) and OCI-Ly19 (B) were dosed by subcutaneous administration with either vehicle control or MLN4924 on the doses and schedules indicated. Mean tumor volume ± SEM are shown (n = 10 mice per group).
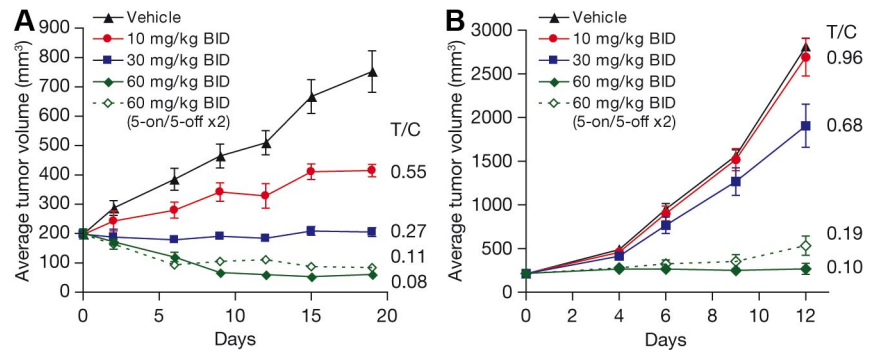
required for antitumor activity. Dosing for 2 cycles of 5 days of treatment followed by 5 days free of treatment did not result in statistically different tumor growth inhibition from continuous daily dosing (T/C = 0.19, $P > .1$). Thus, at the MTD in the OCI-Ly19 model, complete tumor growth inhibition was observed, and this response was maintained when dosing on schedules less than the MTD. The antitumor activity of MLN4924 against OCI-Ly19-luc cells grown disseminated in SCID mice was also assessed and tumor burden quantified using xenogen imaging (supplemental Figure 7). In agreement with the subcutaneous model, dose-dependent tumor growth inhibition was observed, with complete inhibition occurring at 60 mg/kg twice daily with daily dosing. Similarly, dosing for 2 cycles of 5 days of treatment followed by 5 days free of treatment did not result in a statistically different response from continuous daily dosing ($P > .1$).

These data demonstrate that MLN4924 has antitumor activity in xenograft models of ABC- and GCB-DLCBCL. In OCI-Ly10 ABC-DLBCL xenografts, MLN4924 treatment induced tumor regressions (50% reduction in tumor volume), probably through NF-κB signaling inhibition.

MLN4924 inhibits NAE and NF-κB signaling in a primary human DLBCL model resulting in tumor regressions

A primary human DLBCL model (PHTX-22L) was established in SCID-NOD mice that were engrafted subcutaneously with tissue obtained from a 71-year-old man with DLBCL. Mice received single subcutaneous doses of 30 or 60 mg/kg MLN4924; tumor samples were harvested over a 24-hour period to assess pharmaco-dynamic response (Figure 5A-C). Dose- and time-dependent inhibition of NEDD8-cullin levels and elevation of pIκBα levels were observed, with the maximal effect occurring 1 to 4 hours after dose (Figure 5A-B). Elevation of pIκBα levels was similar to that observed in OCI-Ly10 xenografts, suggesting that PHTX-22L xenografts may also have high NF-κB pathway activity. Using the same panel of target genes as in the OCI-Ly10 model, inhibition of NF-κB target gene transcription was detected in PHTX-22L xenografts (Figure 5C). When dosing on a schedule of 3 cycles of 2 days of treatment with 5 days free of treatment, dose-dependent inhibition of PHTX-22L xenograft growth was observed (Figure 5D). The highest dose level of 60 mg/kg twice daily effected tumor regressions on this schedule, which is less than the MTD in this model.

Discussion

MLN4924 is a novel first-in-class NAE inhibitor that has shown potent activity in in vitro and in vivo models of solid tumors.[3] In this report, we characterized the effects of MLN4924 in xenograft models of DLBCL. We showed that MLN4924 has broad tumori-cidal activity across a panel of lymphoma cells and xenograft models, and is able to affect at least 2 distinct mechanisms of action depending on the involvement of NF-κB signaling for cell survival. These data support the ongoing evaluation of MLN4924 in a broad lymphoma patient population and provide rationale for targeted therapy in patients with elevated NF-κB gene signature.[15]

In our studies, there are clear distinctions in the way in which ABC cells respond to NAE inhibition compared with GCB cells. First, analysis of DNA content revealed S-phase accumulation for GCB cells consistent with the induction of DNA rereplication, whereas in G_1 phase, arrest was observed in ABC cells. Second, pIκBα accumulation, inhibition of nuclear p65 levels, and transcrip-tion of NF-κB target genes were noted in ABC cells (OCI-Ly10) but not GCB cells (OCI-Ly19). Third, ABC cells did not undergo DNA rereplication because they did not incorporate BrdU after MLN4924 treatment. Finally, MLN4924 induces apoptosis and tumor regressions in OCI-Ly10 and PHTX-22L xenograft models, which suggests a greater drug sensitivity to NAE inhibition by ABC-type DLBCL cells. Thus, although MLN4924 has potent antitumor activity in both GCB- and ABC-DLBCL models, the different mechanism of action by which these tumor types respond to MLN4924 will allow for appropriate tailoring of MLN4924 clinical development in lymphoma.

Further support for the mechanism of action of MLN4924 on NF-κB in ABC-DLBCL is found in studies using a selective small-molecule inhibitor of IKKβ, ML120B.[17] ML120B was selectively toxic to ABC-DLBCL cells but had no tumoricidal activity against GCB-DLBCL cells, in agreement with the depen-dence of ABC-DLBCL cells on constitutive NF-κB signaling for survival. Analysis of DNA content revealed that OCI-Ly10 and OCI-Ly3 cells accumulate in G_1 on IKK inhibition with ML120B[17] or IκBα superrepressor transfection,[16] similar to the effects ob-served with NAE inhibition. Inhibition of NF-κB target gene transcription using ML120B was effective in OCI-Ly10 and OCI-Ly3 cells, but not in GCB-DLBCL cell lines,[17] again similar to our observations with MLN4924. Recently, it was also demon-strated that inhibition of MALT1 protease activity is selectively toxic to ABC-DLBCL cell lines by virtue of reduced NF-κB signaling highlighting the addiction of these cells to the NF-κB pathway.[20]

We defined the kinetics of CRL substrate accumulation in OCI-Ly10 cells and demonstrated that pIκBα accumulated earlier and at lower inhibitor concentrations than Cdt-1. This supports the hypothesis that NF-κB pathway inhibition by MLN4924 is domi-nant in these cells compared with other cells tested (OCI-Ly19, OCI-Ly7, and other epithelial cells[3]). This is probably a cell-cycle-related phenomenon. For Cdt-1 to accumulate, cells must be
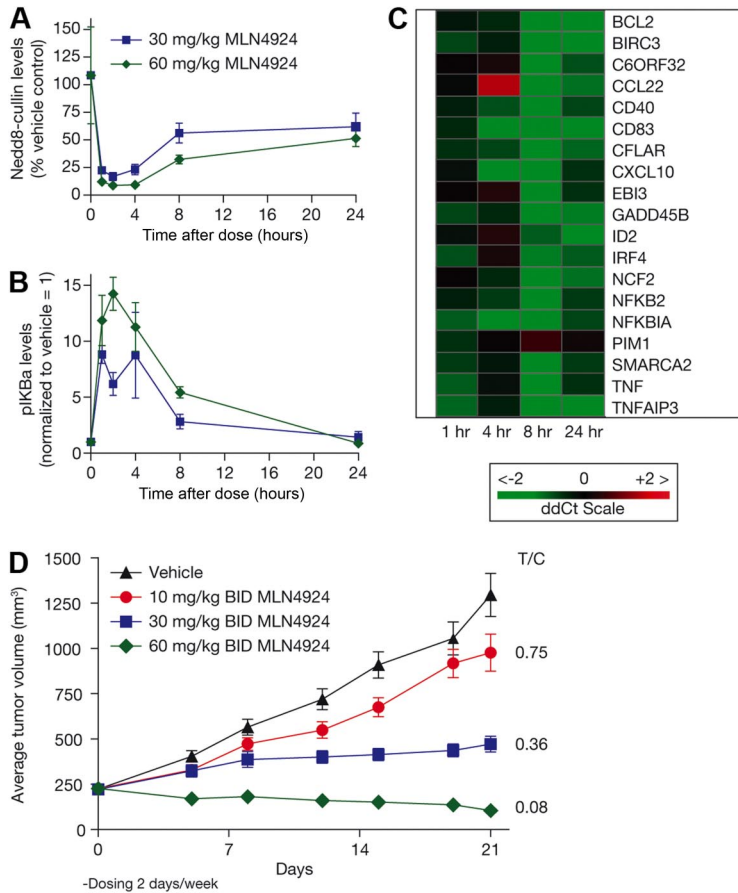
Figure 5. MLN4924 inhibits NAE and the NF-κB pathway and induces tumor regressions in a primary human DLBCL xenograft model. NOD.SCID mice bearing PHTX22L primary human DLBCL xenografts were administered a single subcutaneous dose of vehicle or MLN4924 at 30 and 60 mg/kg. Tumors were excised at the indicated times, and NEDD8-cullin conjugate levels (A) and relative pIκBα levels (B) were measured in the tumor lysates (20 μg protein per lane) by quantitative immunoblot analysis. (C) Quantitative RT-PCR was performed on RNA extracted from tumor samples using human specific primers to measure levels of NF-κB target gene transcripts. (D) NOD.SCID mice were dosed by subcutaneous administration with either vehicle control or on the doses indicated for 3 cycles of 2 days treatment with 5 days rest. Mean tumor volumes ± SEM are shown (n = 10 mice per group).

progressing through the G_1-S phase transition where $CRL1^{Skp2}$ and $CRL4^{DDB1}$ activity for Cdt-1 degradation is highest. In contrast, constitutive activation of IKK in ABC-DLBCL cells appears to be independent of cell-cycle regulation; thus, accumulation of pIκBα occurs in all phases. It is also possible that NAE inhibition has differential effects on individual CRL complexes, with some CRLs being inhibited at lower concentrations than others.

MLN4924 induced tumor regressions in both the OCI-Ly10 cell-line-derived xenograft model and the PHTX-22L model derived directly from a patient biopsy. In contrast, tumor stasis was the maximum response achievable in the OCI-Ly19 xenograft model demonstrating that different treatment outcome may be anticipated for ABC- versus GCB-DLBCL patients. Therefore, in the clinical setting, it will be important to understand NF-κB status of lymphoma to be treated with NAE inhibitors. Such an approach was taken with bortezomib in combination with chemotherapy in DLBCL, with prospective determination showing those patients with ABC- versus GCB-DLBCL having a significantly higher response rate.[21] However, in the same study, bortezomib did not show single-agent activity in either patient population. Because MLN4924 more selectively inhibits protein turnover than bortezomib,[3] MLN4924 may possibly have a more favorable tolerability profile allowing more intense and/or frequent dosing strategies that may demonstrate single-agent activity. In addition, MLN4924 may also have broad activity in the DLBCL population, acting through a combination of both NF-κB inhibition and DNA rereplication mechanisms.

The potent activity of MLN4294 and alternate mechanism of action described for ABC-DLBCL models are not expected to be confined to this disease. Constitutive activation of the NF-κB pathway has been described for a variety of lymphoid malignancies, including MALT lymphoma, primary mediastinal B-cell lymphoma, and Hodgkin lymphoma, plus other lymphoid malignancies.[22-24] NF-κB activation has also been demonstrated in multiple myeloma,[25] Epstein-Barr virus-associated malignancies, primary effusion lymphoma, and adult T-cell lymphoma/leukemia.[23] Genetic lesions in multiple regulators of NF-κB signaling have been identified in lymphoma that can result in constitutive pathway activation. These include somatic mutations in genes that positively (*CARD11*, *TRAF2*, *TRAF5*, *MAP3K7*, and *TNFRSF11A*) and negatively (A20) regulate the NF-κB pathway resulting in constitutive IKK activity.[26-28] In addition, it was recently demonstrated that chronic active BCR signaling is a frequent mechanism of NF-κB activation in ABC-DLBCL.[29] Tumors with these lesions should be sensitive to inhibition of IκBα turnover via blocking NAE and may respond well to MLN4924 treatment. Selective targeting of IKKβ in ABC-DLBCL has proven effective in preclinical models[17]; however, an shRNA screen performed in the context of IKKβ inhibition demonstrated compensatory activation of IKKα-mediated phosphorylation and turnover of IκBα,[30] which could limit the activity of an IKKβ-selective therapy. Activation of noncanonical NF-κB signaling has also been reported in lymphomas.[23] CRL (and hence NAE) activity is involved in the regulation of noncanonical NF-κB signaling[13,14]; we confirm that NAE inhibition can lead to the accumulation of phospho-p105 and a reduction in processing to p50 (supplemental Figure 8) in cells. Thus, NAE inhibition by MLN4924 may also represent a treatment strategy in lymphomas with genetic lesions in the noncanonical NF-κB pathway. Lastly, NF-κB activation in lymphoma can occur

downstream of dysregulated CRL1$^{\beta TRCP}$ turnover of IκBα, including inactivating mutations in IκBα[31,32] and amplifications in c-REL.[23,33] Such genetic lesions would not be susceptible to NF-κB pathway inhibition by MLN4924; experiments are ongoing to determine whether these cells will undergo DNA rereplication.

These studies show that MLN4924 represents a promising agent for the treatment of lymphoma, particularly for those with constitutively activated NF-κB. In addition, the pleiotropic effects of inhibiting CRL-mediated protein turnover in cells may lead to identification of additional subtypes of hematologic malignancies sensitive to NAE inhibition. Finally, because the NF-κB pathway is thought to play an important role in drug resistance to many chemotherapies,[34] MLN4924 used in combination with standard of care agents has the potential to treat a diverse range of malignancies and patient populations.

Acknowledgment

Authorship

Contribution: P.G.S., M.A.M., A.J.B., T.A.S., and S.P.L. participated in the conceptualization and analysis of studies; M.A.M., J.A.-D., M.P.T., U.N., and E.K. performed in vitro cell culture experiments; T.T., J.Z., and M.P.T. performed in vivo antitumor activity and pharmacodynamic experiments; J.Y., E.K., J.J.G., and M.P.T. performed pharmacodynamic analysis experiments; L.M.S., L.D., L.R.D., M.R., M.M., and J.B.B participated in critical discussions of data and reviewed and edited the paper; and P.G.S wrote the paper.

Conflict-of-interest disclosure: All authors (except L.M.S.) were employees of Millennium Pharmaceuticals at the time of these studies. There are no other competing financial interests.

The current affiliation for L.D. is Agios Pharmaceuticals, Cambridge, MA.

Correspondence: Peter G. Smith, Discovery, Millennium Pharmaceuticals Inc, 40 Landsdowne St, Cambridge, MA 02139; e-mail: Peter.G.Smith@MPI.com.

References

1. Brownell JE, Sintchak MD, Gavin JM, et al. Substrate-assisted inhibition of ubiquitin-like protein activating enzymes: the NEDD8 E1 inhibitor MLN4924 forms a NEDD8-AMP mimetic in situ. *Mol Cell*. 2010;37(1):102-111.

2. Soucy TA, Smith PG, Rolfe M. Targeting NEDD8-activated cullin-RING ligases for the treatment of cancer. *Clin Cancer Res*. 2009;15(12):3912-3916.

3. Soucy TA, Smith PG, Milhollen MA, et al. An inhibitor of NEDD8-activating enzyme as a new approach to treat cancer. *Nature*. 2009;458(7239):732-736.

4. Petroski MD, Deshaies RJ. Function and regulation of cullin-RING ubiquitin ligases. *Nat Rev Mol Cell Biol*. 2005;6(1):9-20.

5. Gong L, Yeh ET. Identification of the activating and conjugating enzymes of the NEDD8 conjugation pathway. *J Biol Chem*. 1999;274(17):12036-12042.

6. Fujita M. Cdt1 revisited: complex and tight regulation during the cell cycle and consequences of deregulation in mammalian cells. *Cell Div*. 2006;1:22.

7. Vaziri C, Saxena S, Jeon Y, et al. A p53-dependent checkpoint pathway prevents rereplication. *Mol Cell*. 2003;11(4):997-1008.

8. Karin M, Cao Y, Greten FR, Li ZW. NF-kappaB in cancer: from innocent bystander to major culprit. *Nat Rev Cancer*. 2002;2(4):301-310.

9. Campbell KJ, Rocha S, Perkins ND. Active repression of antiapoptotic gene expression by RelA(p65) NF-kappa B. *Mol Cell*. 2004;13(6):853-865.

10. Ghosh S, Baltimore D. Activation in vitro of NF-kappa B by phosphorylation of its inhibitor I kappa B. *Nature*. 1990;344(6267):678-682.

11. Mercurio F, Zhu H, Murray BW, et al. IKK-1 and IKK-2: cytokine-activated IkappaB kinases essential for NF-kappaB activation. *Science*. 1997;278(5339):860-866.

12. Read MA, Brownell JE, Gladysheva TB, et al. Nedd8 modification of cul-1 activates SCF(beta(TrCP))-dependent ubiquitination of IkappaBalpha. *Mol Cell Biol*. 2000;20(7):2326-2333.

13. Amir RE, Iwai K, Ciechanover A. The NEDD8 pathway is essential for SCF(beta -TrCP)-mediated ubiquitination and processing of the NF-kappa B precursor p105. *J Biol Chem*. 2002;277(26):23253-23259.

14. Fong A, Sun SC. Genetic evidence for the essential role of beta-transducin repeat-containing protein in the inducible processing of NF-kappa B2/p100. *J Biol Chem*. 2002;277(25):22111-22114.

15. Alizadeh AA, Eisen MB, Davis RE, et al. Distinct types of diffuse large B-cell lymphoma identified by gene expression profiling. *Nature*. 2000;403(6769):503-511.

16. Davis RE, Brown KD, Siebenlist U, Staudt LM. Constitutive nuclear factor kappaB activity is required for survival of activated B cell-like diffuse large B cell lymphoma cells. *J Exp Med*. 2001;194(12):1861-1874.

17. Lam LT, Davis RE, Pierce J, et al. Small molecule inhibitors of IkappaB kinase are selectively toxic for subgroups of diffuse large B-cell lymphoma defined by gene expression profiling. *Clin Cancer Res*. 2005;11(1):28-40.

18. Ngo VN, Davis RE, Lamy L, et al. A loss-of-function RNA interference screen for molecular targets in cancer. *Nature*. 2006;441(7089):106-110.

19. Melixetian M, Ballabeni A, Masiero L, et al. Loss of Geminin induces rereplication in the presence of functional p53. *J Cell Biol*. 2004;165(4):473-482.

20. Ferch U, Kloo B, Gewies A, et al. Inhibition of MALT1 protease activity is selectively toxic for activated B cell-like diffuse large B cell lymphoma cells. *J Exp Med*. 2009;206(11):2313-2320.

21. Dunleavy K, Pittaluga S, Czuczman MS, et al. Differential efficacy of bortezomib plus chemotherapy within molecular subtypes of diffuse large B-cell lymphoma. *Blood*. 2009;113(24):6069-6076.

22. Feuerhake F, Kutok JL, Monti S, et al. NFkappaB activity, function, and target-gene signatures in primary mediastinal large B-cell lymphoma and diffuse large B-cell lymphoma subtypes. *Blood*. 2005;106(4):1392-1399.

23. Jost PJ, Ruland J. Aberrant NF-kappaB signaling in lymphoma: mechanisms, consequences, and therapeutic implications. *Blood*. 2007;109(7):2700-2707.

24. Klein U, Dalla-Favera R. Germinal centres: role in B-cell physiology and malignancy. *Nat Rev Immunol*. 2008;8(1):22-33.

25. Ni H, Ergin M, Huang Q, et al. Analysis of expression of nuclear factor kappa B (NF-kappa B) in multiple myeloma: downregulation of nuclear factor kappa B induces apoptosis. *Br J Haematol*. 2001;115(2):279-286.

26. Compagno M, Lim WK, Grunn A, et al. Mutations of multiple genes cause deregulation of NF-kappaB in diffuse large B-cell lymphoma. *Nature*. 2009;459(7247):717-721.

27. Kato M, Sanada M, Kato I, et al. Frequent inactivation of A20 in B-cell lymphomas. *Nature*. 2009;459(7247):712-716.

28. Lenz G, Davis RE, Ngo VN, et al. Oncogenic CARD11 mutations in human diffuse large B cell lymphoma. *Science*. 2008;319(5870):1676-1679.

29. Davis RE, Ngo VN, Lenz G, et al. Chronic active B-cell-receptor signalling in diffuse large B-cell lymphoma. *Nature*. 2010;463(7277):88-92.

30. Lam LT, Davis RE, Ngo VN, et al. Compensatory IKKalpha activation of classical NF-kappaB signaling during IKKbeta inhibition identified by an RNA interference sensitization screen. *Proc Natl Acad Sci U S A*. 2008;105(52):20798-20803.

31. Cabannes E, Khan G, Aillet F, Jarrett RF, Hay RT. Mutations in the IkBa gene in Hodgkin's disease suggest a tumour suppressor role for IkappaBalpha. *Oncogene*. 1999;18(20):3063-3070.

32. Krappmann D, Emmerich F, Kordes U, et al. Molecular mechanisms of constitutive NF-kappaB/Rel activation in Hodgkin/Reed-Sternberg cells. *Oncogene*. 1999;18(4):943-953.

33. Barth TF, Martin-Subero JI, Joos S, et al. Gains of 2p involving the REL locus correlate with nuclear c-Rel protein accumulation in neoplastic cells of classical Hodgkin lymphoma. *Blood*. 2003;101(9):3681-3686.

34. Nakanishi C, Toi M. Nuclear factor-kappaB inhibitors as sensitizers to anticancer drugs. *Nat Rev Cancer*. 2005;5(4):297-309.